BOREAL ENVIRONMENT RESEARCH 14: 971–980
ISSN 1239-6095 (print) ISSN 1797-2469 (online)

Helsinki 18 December 2009

Evaluating the diffuse attenuation coefficient of dry snow by using an artificial light source

Kai Rasmus[1)] and Olli Huttunen[2)]

[1)] *Finnish Environment Institute (SYKE), Jyväskylä Office, P.O. Box 35, FI-40014 University of Jyväskylä, Finland (e-mail: kai.rasmus@ymparisto.fi)*
[2)] *Division of Geophysics, Department of Physical Sciences, P.O. Box 64, FI-00014 University of Helsinki, Finland; current address: Luode Consulting Ltd., Olarinluoma 15, FI-02200 Espoo, Finland*

Received 12 Oct. 2007, accepted 28 Jan. 2009 (Editor in charge of this article: Timo Huttula)

Rasmus, K. & Huttunen, O. 2009: Evaluating the diffuse attenuation coefficient of dry snow by using an artificial light source. *Boreal Env. Res.* 14: 971–980.

A novel and non-destructive method is proposed for measuring the diffuse attenuation coefficient (K_d) of snow which helps to solve the problem of snow cover disturbance whilst making the measurements. The method is based on the measurement of backscattered upwelling light from an artificial light source above the snow cover. A Monte Carlo model of this measurement system was developed and model runs were made with different sized snow grains. The model produced results that show that the K_d obtained from the new method is higher than the K_d that would be obtained using vertical profiles of downwelling irradiance. The coincidence is better for larger grain sizes. A pilot study of the new measurement system was made in Kilpisjärvi in northern Finland in early January 2003. The measurement results for dry snow show that in the visible wavelengths the attenuation coefficients obtained are in reasonable agreement with those obtained using more traditional methods for snow with similar properties. However, in the near infrared the values are much lower.

Introduction

Solar radiation is one of the most important terms in the heat budget of snow. The albedo and the diffuse attenuation coefficient (K_d) are the properties of the snow that describe the way in which radiation is available within the snow at each depth. The theory behind the attenuation of light in snow is reasonably well understood (Warren 1982) but due to snow being a mixture of air and ice grains, the attenuation of light in snow is very hard to measure without disturbing the snowcover. Several approaches to this measurement problem exist that disturb the snow to a lesser or a greater extent. The crudest method is to measure the irradiance in the snow from the side of a snow-pit but this method produces the largest disturbance. To reduce its effect, the pit can be covered with snow before the measurements take place. Another way is to set the instruments up before the snowcover forms so the snow can form on top of them. This method needs a lot of time (Perovich 2007) and the snow above the measurement setup is not necessarily in the same state as the surrounding snow cover. A good and widely used way of measuring K_d is to first measure the attenuation of upwelling radiation by pushing a probe into the snow from above and then deducing the value of K_d from the obtained profile (Kärkäs *et al*. 2002,

Warren *et al*. 2006). This method assumes that the upwelling radiance profile is related to the downwelling irradiance profile at all depths in a well known way. This assumption is acceptable because after a few centimetres the light distribution within small grained snow becomes diffuse. In addition to the diffuse attenuation coefficient of upwelling light, the value of K_d can be deduced from the transmittance, the ratio of transmitted to incident light, of snow samples (Beaglehole *et al*. 1998). The transmittance then needs to be related to K_d in some way.

For sea or lake ice, the value of K_d can be calculated from under-ice measurements of irradiance. The instrument can be placed under the ice and snow without disturbing the snow (Rasmus *et al*. 2002). The effect of the ice and the thin layer of water between the ice and the instrument can be subtracted from the measured signal to leave only the effect of the snow cover itself. Recent measurements of the attenuation coefficient of snow above sea ice have been made by Hamre *et al*. (2004). These were made by measuring the attenuation of light in the snow covered sea-ice system and fitting a radiative transfer model to the measurements. Haines *et al*. (1997) used upwelling light from an artificial light source below the ice to measure the value of K_d in sea ice.

All of the above methods make the measurement of K_d and the construction of time-series of the same snow very difficult. Only the under-ice methods are totally non-destructive as far as the snow being measured directly at the measurement location is concerned. In this study a novel, totally non-destructive, method for measuring the K_d based on the backscattered upwelling light from an artificial light source above the snow surface is presented. The method is non-destructive because the measurement head does not need to be inserted into the snow. The upwelling light from the snow depends on the physical properties of the snow.

Here, a presentation of radiative transfer in snow is followed by the introduction of a new measurement concept, and finally its feasibility is studied using a two dimensional Monte-Carlo radiative transfer model to simulate the system. Comparisons between K_d and the variable value obtained using the new system are then made. Then results from a measurement implementation of the method for dry snow are shown for a pilot study from Kilpisjärvi in the northwestern tip of Finland. Comparisons with the measured K_d value and values obtained by other authors using different methods are made.

Radiative transfer of light in snow

Radiance is the amount of radiative energy incident per unit time in a unit spectral bandwidth, per unit area of surface from a solid angle:

$$L_\lambda = L_\lambda(z,\theta,\phi), \quad (1)$$

where θ and ϕ are the declination and azimuth angles describing the direction of the radiation. The subscript indicates that the quantity has a wavelength dependence. The subscript will be left out from this point on but the wavelength dependence is still implied in all quantities.

L can be integrated over all directions in a hemisphere to produce fluxes of radiation. These fluxes are called irradiances. If L is integrated over the upper hemisphere the product is the downwelling irradiance (E_d):

$$E_d(z,\theta,\phi) = \int_0^{2\pi}\int_0^{\frac{\pi}{2}} L(z,\theta,\phi)\cos\theta\,\sin\theta\,d\theta\,d\phi. \quad (2)$$

Similarly if the integration is made over the lower hemisphere, the result is the upwelling irradiance (E_u):

$$E_u(z,\theta,\phi) = -\int_0^{2\pi}\int_{\frac{\pi}{2}}^{\pi} L(z,\theta,\phi)\cos\theta\,\sin\theta\,d\theta\,d\phi. \quad (3)$$

The distribution of radiation within a medium is described by the radiative transfer equation. In this equation the radiation in a beam of radiation decays due to absorption and scattering from the beam and increases due to emission or scattering into the beam. The equation can be written in a simplified form as:

$$\frac{\partial L(z)}{\partial s} = -cL(z) + \int_0^{4\pi}\beta L(z')\,d\Omega'', \quad (4)$$

where c is the beam attenuation coefficient, Ω is a solid angle and β is the volume scattering function. The second term on the right-hand side in Eq. 4 is a source term related to scattering

into the beam of radiation. The beam attenuation coefficient is the sum of the absorption and scattering coefficients. The solution to Eq. 4 depends on the boundary conditions and the scattering source term. The boundary conditions depend on the system under consideration but for the top surface it is usually the illumination.

In a horizontally homogeneous snowpack and for a diffuse radiation field, which begins a few centimetres below the surface (Warren 1982), the radiative transfer equation can be reduced to predict exponential decay if the scattering source term is assumed to also decay exponentially. The K_d of light for the downwelling irradiance (E_d) can then be calculated. It is:

$$K_d(z) = -\frac{1}{dz} \ln E_d(z), \qquad (5)$$

where λ is the wavelength and z is the depth. If the value of K_d is known, then the vertical light profile within the snow can be calculated and used in thermodynamic modelling. If a profile of vertical radiation measurements is available then it can be used to calculate K_d using Eq. 5. Similarly the diffuse attenuation coefficient for upwelling irradiance (K_u) can be obtained by using E_u in place of E_d in Eq. 5.

The two most important phenomena that define the ultraviolet (UV), visible (VIS) and near infrared (NIR) radiation distributions within the snowpack are absorption and scattering. For snow, emission does not generally play a major role at these wavelengths of natural light. The absorption coefficient of ice has a minimum in the blue wavelengths and increases as the wavelength both increases and decreases from that waveband value. The increase with wavelength is five orders of magnitude across the solar spectrum from 500 to 2000 nm and two orders of magnitude within the VIS and near UV wavelengths (Warren *et al*. 2006). Because of this increase, the probability of absorption of photons in the snowpack after multiple-scattering events increases substantially with wavelength. The mean path-length between scattering events of photons at 2000 nm is only 0.1 mm, and so most of the photons that escape from the top of the snowpack at these wavelengths do so after only one scattering event. Whilst this is true in the mean, some photons do propagate onwards into the snowpack after the first scattering event. Across the visible spectrum, the absorption coefficient does vary, but it is so small everywhere that almost no absorption occurs during the transit of light through individual snow grains and so the exiting light consists mostly of photons scattered numerous times in the snow.

Photons enter the snowpack and are scattered around until they are either absorbed or they emerge from the snowpack. Snow grains scatter light in a very strongly anisotropic way with most of the scattering occurring in forward directions. The amount of forward-scattered light becomes larger when the grain size increases. In addition to this, photons that go through coarse-grained snow have to pass through a larger volume of ice between scattering events, and so they have a larger probability of being absorbed. In visible wavelengths, the absorption coefficient of ice is very small, and so this effect becomes much less important.

Forward scattered photons penetrate deep into the snow when they arrive with high incidence angles (e.g. when the solar elevation is high). Many scattering events are required for these photons to eventually escape the snowpack from the top surface. The emerging photons are therefore distributed more uniformly with angle into the upward hemisphere than is the case for lower incidence angles.

New method for measuring K_d

If the illumination comes from a cone of light (*see* Figs. 1 and 2) then the boundary conditions of the system become more complicated. The illumination is the top boundary condition up to $x = x_S$ after which there is no light coming from above. The radiation flux passing horizontally through x_S is a boundary condition for the solution beyond x_S. The other boundaries are radiating boundaries at the bottom and at the top after $x = x_S$. The snow can be considered infinite in the x-direction.

The light entering into the snow after $x = x_S$ would decay as it passes further into the snowpack. A certain portion of it would be absorbed, but the rest would continue until it exits the snowpack at the top or bottom boundary. The radiation leaving the top boundary would there-

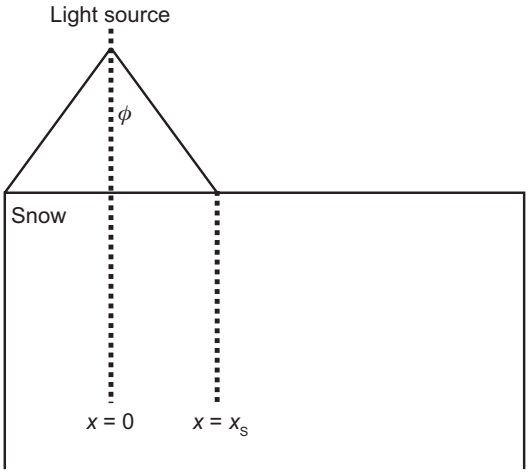

Fig. 1. Schematic of the snow cover when illuminated from above with a cone of light.

Fig. 2. Measurement setup. Upwelling light can be seen as a light gray area beyond the illuminated snow patch (photograph by Olli Huttunen).

fore depend on the absorption and scattering properties of the snow and a certain coincidence between the attenuation coefficient of the horizontal profile of this upwelling light and K_d would be expected. The presence of an open top boundary would mean that a photon in horizontal propagation has a larger probability of exiting the snow cover. This would lead to the decay coefficient for upwelling irradiance in the horizontal direction being larger than K_d.

This gives the motivation to define a new variable that describes the horizontal attenuation of upwelling irradiance at the surface. It will be called K_x and will follow the formula for K_d shown in Eq. 5:

$$K_x(x) \equiv -\frac{1}{dx} \ln E_u(x), \qquad (6)$$

where z is the depth. In this study, the definition of K_x will be applied after $x = x_S$.

The horizontal profile of upwelling irradiance can be measured without disturbing the snow cover. This means that by measuring the value of K_x and studying the relationships between it and K_d, the value of K_d for snow can eventually be deduced in a non-destructive manner.

Modelling

The system (shown in Figs. 1 and 2) requires a numerical solution to the radiative transfer equation due to the complicated nature of the boundary conditions. A Monte-Carlo numerical approach was chosen because it is capable of coping with them.

Monte-Carlo model

Monte-Carlo modelling refers to a technique initially developed by Metropolis and Ulam (1949) to simulate physical processes using a stochastic model. In the case of radiative transfer, it calculates the radiation field using a large number of simulated photons called scatterees that pass through, and interact with, a medium. As an example, the Monte-Carlo method is also rapidly becoming the main way of modelling light transfer in such media as tissue (Prahl *et al*. 1989). Light *et al*. (2003) used Monte Carlo modelling to study the light field within the sea ice.

In this modelling study, snowpack is assumed to be semi-infinite in the vertical direction, infinite in the x-direction, homogeneous and consisting of spherical snow grains. The diameter of the grains is an input variable to the model.

The model calculations start by selecting evenly distributed random numbers P_n in the range [0,1] which are related to model parameters using the following equations. The initial

direction (θ_0) from nadir taken by the scatteree is calculated from:

$$P_1 = \frac{2}{\pi}\theta_0 + \frac{1}{2}. \quad (7)$$

The horizontal location of the scatteree on the surface of the snow is fixed by the initial angle and the height of the light source (H). No scatteree interactions in the air between the lamp and the surface are allowed to occur.

When the scatteree hits the surface of the snow it travels a distance less than one free length (L). L is also the distance between interactions:

$$P_2 = \frac{L}{2d}, \quad (8)$$

where d is the diameter of the snow grain. In the parameterization used in this study the maximum free length is assumed to be equal to two times the diameter of the snow grains at nominal snow densities of 400 kg m^{-3}. This produces an attenuation coefficient of 500 m^{-1} for grains with a diameter of 1000 μm because L is the reciprocal of c (i.e. $L = c^{-1}$). The free length also decreases with grain size. In dry snow with small grains, the snow is relatively compact and the free space between grains is assumed to be roughly equal to the grain diameter. This parameterization removes the necessity of an *a priori* assumption of c.

The fate of the scatteree at the point of interaction is then decided.

$$P_3 \geq \varpi \rightarrow \text{absorption}, \quad (9)$$

where ϖ is the single scattering albedo which is the ratio of the scattering coefficient to c. In this study, ϖ is taken to describe the distribution of scatteree interaction events between scattering and absorption. If it is close to one, then most of the events are scattering events and only a very small amount of interactions are absorption events. This is reflected in the fact that the random numbers are uniformly distributed. If ϖ is close to one it is very improbable that absorption occurs. If absorption does occur, ie the value of P_3 is larger than ϖ, then the scatteree is terminated and the calculation restarts from Eq. 6 with the next scatteree.

The scattering or declination angle (θ) away from the direction the scatteree is travelling in is then calculated from:

$$P_4 = \int_0^{\theta} \overline{p}(\theta')\, d\theta', \quad (10)$$

where p is the normalised phase function. The phase function determines the probability distribution of the directions into which a photon can be scattered. It is assumed to be symmetrical with regard to the azimuth angle but because this model setup is two-dimensional (x–z) the scattering direction has to be projected onto the x–z plane according to the value of the azimuth angle. This leads to the total projected direction change in the x–z plane (θ_c) experienced by the scatteree.

$$P_5 = \frac{1}{\pi}\arcsin\left(\frac{\theta_c}{\theta}\right) + \frac{1}{2}, \quad (11)$$

θ_c is added to the direction in which the scatteree was travelling to get a new propagation direction. Equation 11 is not valid for a scattering angle of 0°, but for this angle the projection does not need to be made.

In this study the Henyey-Greenstein phase function is used:

$$p(\cos\theta) = \varpi \frac{(1-g^2)}{(1+g^2-2g\cos\theta)^{\frac{3}{2}}}, \quad (12)$$

where g is the asymmetry parameter which is the first moment of the Mie-scattering phase function when it is developed into a series of Legendre polynomials. Equation 12 is normalised to one and used in Eq. 10. In the original study by Henyey and Greenstein (1941) on diffuse radiation in the galaxy, the phase function is related to the spherical albedo. In this study, that has been changed to the single-scattering albedo because the incident light is not isotropic. The exact specifics of the reflectance distribution are not being studied so the use of the Henyey-Greenstein approximation to the phase function is plausible.

The model run starts with the calculation of the initial direction of the scatteree from the point source at height H using Eq. 7. This is used together with H to determine the initial x-location on the snow surface. For this study, H is set to a value of 40 cm. The scatteree is then

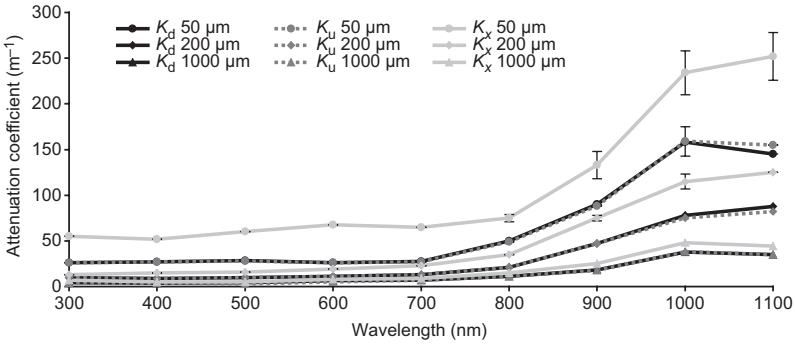

Fig. 3. Modelled mean values of K_d, K_u and K_x for different grain sizes after five model runs. The number in the legend indicates the grain size in micrometers. The error bars indicate one standard deviation.

added to the downwelling flux at the surface. The free length before the first interaction is then calculated using Eq. 8. The next step is to determine whether scattering or absorption occurs. If the scatteree is absorbed then the calculations continued from the beginning with a new scatteree. If the scatteree is scattered then the new propagation direction is calculated by adding the scattering angle obtained form Eqs. 10 and 11 to the old propagation direction. The calculations continue with the calculation of the free length before the next interaction event. At certain depths, the scatteree is added to the downwelling flux, or upwelling flux if it is travelling in the upward direction. If the scatteree exits the snow cover at the top surface, it is added to the upwelling flux at the surface and the calculation continues with a new scatteree. No backscattering from the atmosphere is assumed. In clear-sky cases this assumption is acceptable even though cloudcover considerably increases the chance of a photon being scattered back to the surface. However, the clouds are usually so far away that a photon originating from the artificial light source that exits the snow cover and is scattered from the clouds has very little chance of ending up in the study region again.

The model was run for grain sizes of 50, 200 and 1000 μm and for wavelengths between 300 and 1100 nm with a 100 nm spacing. The parameters g and ϖ were taken from the Mie calculations of Wiscombe and Warren (1980). The number of scatterees was set to 1×10^5 and five runs were made for each combination of parameter values. For 200 μm, the calculations were repeated for 1×10^7 scatterees but the results were not significantly improved. The half-angle of the lamp opening was set to 45° initially but a second set of model runs were made using an opening of 22.5°. For the second set of runs, Eq. 7 was modified to restrict the initial direction to a smaller range of angles:

$$P_1 = \frac{4}{\pi}\theta_0 + \frac{1}{2}. \quad (13)$$

After the model runs were made, the values of K_d were calculated by fitting a straight line to the profile of the natural logarithm of the downwelling flux using values up to a depth of ten cm. The value of K_x was similarly calculated from the upwelling flux values at the surface starting from the edge of the illumination. Only values further than 20 cm away from the centre of the light source in the horizontal direction were used to be sure that the area was not affected by direct downwelling light from the source of scatterees.

Model results

The modelling results show that the smallest grains have the highest values of K_d, K_u and K_x and the largest differences between K_d and K_x. The modelled mean K_d, K_u and K_x values from the five runs together with the standard deviations (Fig. 3) show that the spectrum for K_x for 50 μm grains at the highest wavelengths has the highest standard deviation. Snow with grains of 50 μm size is usually not found in boreal regions or in the coastal zone of Antarctica (Kärkäs *et al*. 2002).

The ratio of K_x to K_d becomes closer to unity for larger grain sizes in the visible wavelengths (Fig. 4). In the near infrared, the ratio of K_x to K_d becomes almost one for large grains.

The values of the ratios of K_u to K_d are one for all grain sizes and all wavelengths (Fig. 4).

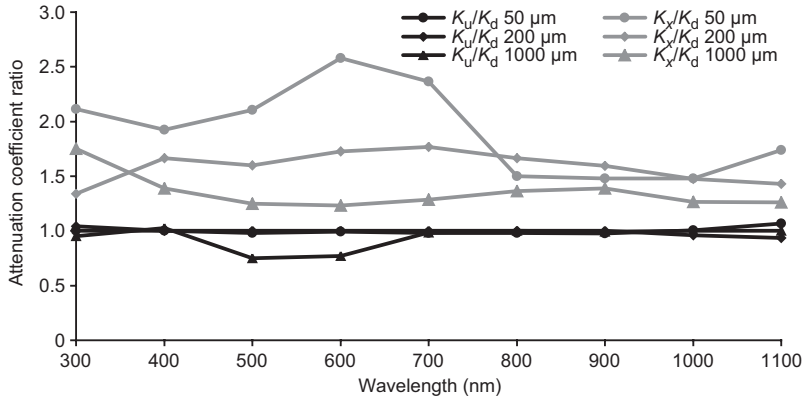

Fig. 4. Calculation results for different grain sizes, showing the ratio of K_u to K_d and the ratio of K_x to K_d. The number in the legend indicates the grain size in micrometers.

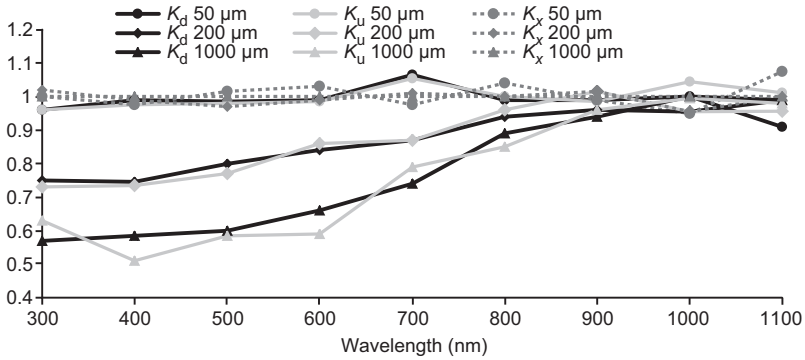

Fig. 5. Ratio of the attenuation coefficients for a lamp opening of 22.5° to a lamp opening of 45°.

The consequence of this is that the deduction of K_d using upwelling radiation is capable of producing reasonable results.

The model runs for a half-angle lamp opening of 22.5° showed attenuation coefficients that were very similar to the 45° case. The ratios of attenuation coefficients at 22.5° to attenuation coefficients at 45° are close to unity at all wavelengths and all grain sizes (Fig. 5). The ratio is smallest for large grains at short wavelengths. For the smallest grain sizes the two different model runs produced almost identical results. The ratios become unity after 900 nm for all grain sizes.

The ratios of calculated upwelling to downwelling flux can be considered to be equal to the albedo, which is the ratio of E_u to E_d. The albedo increases as the grain size decreases and decreases as the wavelength increases (Fig. 6). These variations are similar to variations in albedo observed in measurements of dry snow in e.g. Antarctica (Pirazzini 2004, Rasmus 2006). This is an indication that the model can be used to simulate the radiative transfer in the snow.

Case study

Measurement setup

A pilot study of this measurement setup was made on the snow above the ice of Kilpisjärvi, a lake in northern Finland (69°03´N, 20°50´E) in the late evening in the beginning of January 2003. The air temperature was –30 °C and there was darkness. The snow grains at the site were found to be approximately 1000 μm in length but they were not round, being more needle-like which is not ideal for comparisons with the model. The snow was assumed to be relatively dry.

The snow was illuminated from above using a halogen lamp at a height of 40 cm (Fig. 2). The lamp had a shade to limit the illumination into an angle of approximately 40°. This is five degrees less than in the model runs but due to the width of the real lamp it was not a genuine point source and some light was emitted outside the lamp opening. The lamp spectrum was continuous in the visible and near infrared wavelengths.

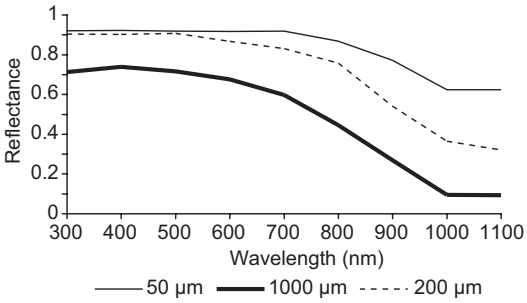

Fig. 6. The ratio of the calculated upwelling and downwelling fluxes below the lamp for different grain sizes. This can be called the reflectance of the snow cover.

The irradiance measurements were made using a Li-Cor LI1800UW spectroradiometer. The LI1800UW is a good instrument for this kind of measurement because it scans the whole spectrum of radiation with one photodiode using a rotating bandpass filter and a rotating interference filter to split the irradiance into wavebands with a resolution of 6 nm. This makes it very sensitive to small radiation values. The integration time of the instrument was 40 s for the whole spectrum between 300 and 1100 nm. In this study the length of the integration time was not a problem because the light source was constant. It was actually a benefit because of the low light levels. A remote cosine corrector fitted to the end of a fibre-optic cable was used to make the measurements directly at the surface.

The downwelling irradiance was measured below the light source and then the upwelling irradiance was measured at 0, 25, 50 and 100 cm away from the centre of the light source. Two spectra of light were measured at each location. Only digital numbers (DN) were used in the calculations because only relative values of irradiance were of interest.

Measurement results

The downwelling and upwelling surface fluxes at point 0 (under the light source) together with the upwelling surface fluxes at three points going away from the light source show that the spectra are evenly spaced between 0 and 50 cm (Fig. 7). This indicates exponential decrease for the evenly spaced (in x) spectra. At 100 cm away from the light source the decrease is no longer the same because the change in x is double to that of the previous steps. The instrument is already close to its digital resolution so this could be a reason for the change in K_x values. Other sources of error include the spatial variations in the illumination due to the non-ideal shape of the lamp and the shape of the grains being non-spherical.

Equation 6 was used to calculate the values of K_x for the different steps. They are almost independent of wavelength in the visible band and the near infrared (Fig. 8). The K_d for the 0–25 cm step shows a slight increase towards the longer wavelengths following the shape of ice absorption.

Discussion

According to the Monte Carlo modelling results, the value of K_x is larger than the K_d for the chosen lamp geometry. The overestimation is largest for the smallest grains. This is because of the higher

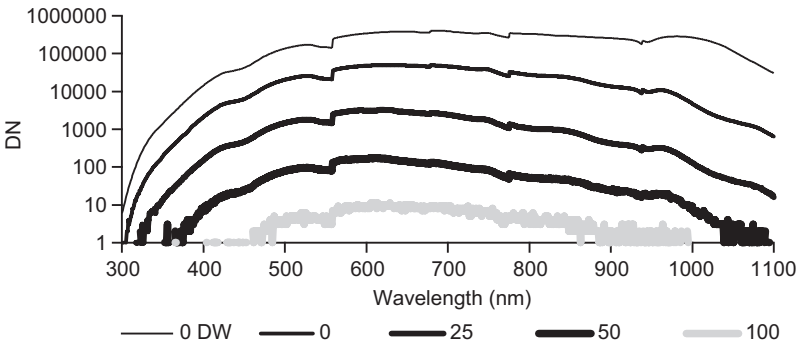

Fig. 7. The downwelling and upwelling flux below the light and at several distances away from it.

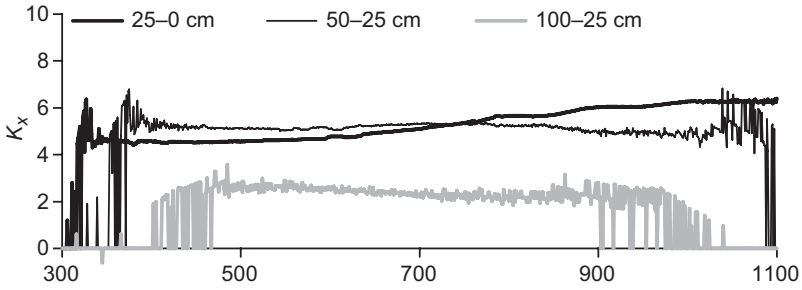

Fig. 8. K_x calculated for different measurements.

probability for photon escape into the atmosphere whilst in horizontal propagation due to the constant presence of the open top snow surface.

Photons entering the snowpack at the edge of the illuminated area do so at a larger zenith angle. Therefore, as the large grains scatter them mainly in a forward direction they have a good chance of escaping the snowpack further away from the light source after a few scattering events. Photons are scattered more diffusely from small grains and so they are more likely to emerge from the snowpack closer to the light source. The results for the smallest grains show that the effect of making the lamp opening smaller is negligible. However for larger grains, making the opening smaller, and thus making the zenith angle of the incident photons smaller, has a dramatic effect at short wavelengths. The value of K_d is almost halved. Photons approach the surface of the snow at a steep angle, penetrate deep into the snowpack and have a very small chance of escaping from the snowpack again.

The 200 μm modelled values of K_x correspond to those measured by Beaglehole *et al.* (1998) for K_d. They deduced K_d from transmission values and obtained values between 12 and 30 m^{-1} at 400 nm and between 20 and 35 m^{-1} at 700 nm for Antarctic snow.

The attenuation coefficient obtained for a mean snow grain size of 1000 μm measured in the coastal zone of Antarctica at 470 nm using a vertical profile of upwelling radiance was found to be 11 m^{-1} (Kärkäs *et al.* 2002). The measurement results for the value of K_x obtained in this study are approximately half of that value as are the modelled results for 1000 μm grains. The modelled K_x values at 200 μm were however the same as in the measurements of Kärkäs *et al.* (2002). The grain size measurement in Kärkäs *et al.* (2002) was based on a small sample size and the grain size measurements are probably an overestimation of the real grain size.

The measurement results from the pilot study show a reasonable coincidence with the attenuation coefficient results of Warren *et al.* (2006) between wavelengths of 300 and 600 nm. They sampled Antarctic snow with a grain size of between 50 and 200 μm. The snow in the pilot study had larger grains which should produce a lower attenuation coefficient. The measured attenuation coefficient in this study seems to underestimate the value of K_d. Measurement results in this study could be affected by impurities within the snowpack whilst Warren *et al.* (2006) made their measurements in clean Antarctic snow. Even though the snow is visually devoid of impurities, they can be present in concentrations too small to be visible by the naked eye. Even these small concentrations can have had an effect on the results.

The measured K_x values are much less than values of K_d for snow obtained by Hamre *et al.* (2004). Their measurements were of snow above a sea-ice cover and the calculations were made by measuring the light transmitted through the whole snow–sea-ice system and removing the effect of sea ice. This is a totally different type of environment so the comparison is not trivial to make. For example, shallow snow on sea ice is subject to brine and heat from the sea ice below.

In the visible wavelengths, the measured values of K_x are slightly lower than the values for new snow measured by Perovich (2007) but the spectral shape is not the same. In the near infrared wavelengths the measured values from this study are much lower.

This method of deducing K_d from measurements of K_x is totally non-destructive on dry

snow and so the same snow can be sampled repeatedly. This makes the construction of time-series of K_d of the same snow possible to construct. The measurements in this study are the first such measurements of the upwelling light of an artificial light source from snow. The measurement setup requires relative darkness, or very sensitive instruments, which can limit its usefulness on measurement campaigns to for example Antarctica during the Austral summer.

The model results show that the method presented could be a new way to calculate the K_d of snow. The measurements in this study represent a pilot study of the method but still show that the method produces values of K_x which are broadly similar to those of K_d. More measurements, maybe with different illumination geometries, are required before a firmer conclusion can be made.

Conclusions

In this study a new, non-destructive method for measuring light attenuation in snow was proposed. The method requires a horizontal surface profile of upwelling irradiance from a conical artificial light source from which K_d can be deduced. Modelling results from a Monte Carlo radiative transfer model and measurement results for one dry snow location in Finland were presented. The model results show that K_d obtained from the new method is higher than K_d that would be obtained using vertical profiles of E_d at all wavelengths. The coincidence between the two different values of K_d becomes better for larger grain sizes. For large grain sizes, smaller values of K_d for upwelling and downwelling radiation are produced when the opening of the lamp is made smaller. The K_x value did not show any sensitivity to the opening angle of the lamp. In the visible wavelengths the results show that the measured K_x values obtained were in reasonable accordance with K_d values obtained by other authors for snow with similar properties. In the near infrared the measured results were too low but the method produces an overestimated value for the value of K_d in the visible wavelengths. More measurement results are required to make a firm conclusion of the validity of the method. The measurements in this study are the first measurements of the upwelling light produced by an artificial light source in snow.

Acknowledgements: The authors wish to thank the Division of Geophysics at the University of Helsinki for giving the possibility to do the field work. The Kilpisjärvi biological station of the University of Helsinki is thanked for providing logistical support and housing the expedition during the harsh conditions of the Arctic winter.

References

Beaglehole D., Ramanathan B. & Rumberg J. 1998. The UV to IR transmittance of Antarctic snow. *J. Geoph. Res.* 103(D8): 8849–8857.

Haines E.M., Buckley R.G. & Trodahl H.J. 1997. Determination of the depth dependent scattering coefficient in sea ice. *J. Geophys. Res.* 102: 1141–1151.

Hamre B., Winther J.-G., Gerland S., Stamnes J.J. & Stamnes K. 2004. Modeled and measured optical transmittance of snow-covered first-year sea ice in Kongsfjorden, Svalbard. *J. Geoph. Res.* 109: C10006, doi:10.1029/2003JC001926.

Henyey L.G. & Greenstein J.L. 1941. Diffuse radiation in the galaxy. *Astrophys. J.* 93: 70–83.

Kärkäs E., Granberg H.B., Kanto K., Rasmus K., Lavoié C. & Leppäranta M. 2002. Physical properties of the seasonal snow cover in Dronning Maud Land, East-Antarctica. *Ann. Glaciol.* 34: 89–94.

Light B., Maykut G.A. & Grenfell T.C. 2003. A two-dimensional Monte Carlo model of radiative transfer in sea ice. *J. Geoph. Res.* 108: C3219, doi: 10.1029/2002JC001513.

Metropolis N. & Ulam S. 1949. The Monte Carlo method. *J. Am. Stat. Ass.* 44: 335–341.

Perovich D.K. 2007. Light reflection and transmission by a temperate snow cover. *J. Glaciol.* 53: 201–210.

Pirazzini R. 2004. Surface albedo measurements over Antarctic sites in summer. *J. Geophys. Res.* 109: D20118, doi: 10.1029/2004JD004617.

Prahl S.A., Keijzer M., Jacques S.L. & Welch A.J. 1989. A Monte Carlo model of light Propagation in tissue. *SPIE Institute Series* IS 5: 102–111.

Rasmus K., Ehn J., Granskog M., Kärkäs E., Leppäranta M., Lindfors A., Pelkonen A., Rasmus S. & Reinart A. 2002. Optical measurements of sea ice in the Gulf of Finland. *Nordic Hydrology* 33: 207–226.

Rasmus K. 2006. Field measurements of the total and spectral albedo of snow and ice in Dronning Maud Land, Antarctica. *Geophysica* 42: 17–34.

Warren S.G. 1982. Optical properties of snow. *Reviews of Geophysics and Space Physics* 20: 67–89.

Warren S.G., Brandt R.E. & Grenfell T.C. 2006. Visible and near-ultraviolet absorption spectrum of ice from transmission of solar radiation into snow. *Appl. Opt.* 45: 5320–5334.

Wiscombe W.J. & Warren S.G. 1980. A model for the spectral albedo of snow. I: pure snow. *J. Atmos. Sci.* 37: 2712–2733.